GeoScience Engineering

REPROCESSING OF REGIONAL 2D MARINE SEISMIC DATA OF PART OF TARANAKI BASIN, NEW ZEALAND USING LATEST PROCESSING TECHNIQUES

Olawale Olakunle OSINOWO[1,2]
[1]*Imperial College London, Department of Earth Science and Engineering, United Kingdom*
[2]*University of Ibadan, Department of Geology, Ibadan, Nigeria*
E-mail: olawale.osinowo13@alumni.imperial.ac.uk or wale.osinowo@ui.edu.ng

ABSTRACT

This study employed the use of various newly developed seismic data processing techniques, which had not been available as at the time (1986) of acquisition of the regional 2D marine seismic data (TRV 434) of part of Taranaki Basin, New Zealand, to reprocess the data in order to improve the seismic volume as well as the quality of subsurface information derivable from the data which remain one of the vital sources of information for the preliminary insight for petroleum prospect evaluation of the basin. The reprocessing operations attenuated various unwanted signals associated with the seismic data, F – K transform filter filtered out low frequency noise including swell noise, while other noise types embedded in the seismic data were attenuated using Time Variant Omsby-Bandpass filters. Predictive deconvolution attenuated water bottom multiples as well as other periodic unwanted signals. True amplitude recovery technique restored lost reflection energies and made deeper reflections visible. Post and Pre-Stack Time Kirchhoff migration (PSTM) techniques appropriately repositioned dipping reflection events to their appropriate locations in time and space. Diffraction curves were collapsed to improve data resolution of both the shallow and deep reflection events. The reprocessing activities generally increased the illuminating strength of the TRV 434 marine seismic data to image the subsurface of the surveyed part of Taranaki Basin, which presented complex subsurface geology in terms of structures and rock association.

Keywords: Kirchhoff migration; Omsby-Bandpass filters; Swell noise; Taranaki Basin; Velocity analysis.

1 INTRODUCTION

The Taranaki Basin in New Zealand is the only basin as at present with known commercial accumulation of hydrocarbon and thus occupies an important role in the hydrocarbon potential development of the country. The geological processes that resulted in the generation and preservation of hydrocarbon in this basin are complex and thus intricate to understand in terms of identification of hydrocarbon traps, many of which are subtle and difficult to map [1]. The role of clear and precise subsurface image in identifying subtle hydrocarbon traps can, therefore, not be overemphasised for effective hydrocarbon prospect generation, especially in a region with lack of surface outcrops that can expose a lead. This study therefore desires to reprocess the regional 2D marine seismic data of part of Taranaki Basin, acquired in 1986 with the object of improving the seismic data's ability to image the subtle subsurface images as well as remove some ambiguities relating to the interpretation of the data as a result of unclear seismic information extracted from the data. The data re-processing employs the present-day processing techniques which were not available as at the time of original data acquisition, to re-process the seismic data in order to increase signal resolution and thus enhance subsurface information that could be extracted from the data. The re-processing work flow attenuates noise and other undesired seismic energies to the barest minimum, recovered lost primary energies, enhances weak signals as well as improves the resolution of the data by migrating the dipping events to the appropriate positions in time and space using post and pre-stack migration algorithms.

2 GEOLOGICAL OVERVIEW OF TARANAKI BASIN

Taranaki Basin is a wedged shaped foreland sedimentary basin located mainly offshore west of the North Island of New Zealand but also extends onshore to the Taranaki Peninsula. The basin covers an area of 100,000 km^2, with the offshore making up to 80 % of the total area. It extends for 350 km in the north-south direction and consist of up to 8 km thickness of Late Cretaceous and Tertiary strata [2]. The basin is bound in the east by the Taranaki Boundary Fault System which extends from Nelson in the South Island to the area west of Kawhia Harbour, Western North Island. In the south-west, the basin is limited by the Challenger Plateau, but the north-western limit of the basin is not clearly defined [3].

The formation of the basin started with rifting in the Late Cretaceous and was transformed through and affected by series of tectonic activities such as passive subsidence, compressional tectonics and the late back-arc rift [1, 4]. Three episodes of tectonic activities affected the basin and left visible evidence of deformation in the Taranaki Basin, namely; the Late Cretaceous to Palaeocene extension, Late Eocene to Miocene shortening, and Pliocene to Holocene extension (Figure 1). Four main stratigraphic sequences have been mapped in the basin (Figure 2), and they are the Late Cretaceous syn-rift sequence, Palaeocene-Eocene Late-rift and post-rift transgressive sequence, Oligocene-Miocene fore deep and distal sediment-starved shelf and slope sequence, Miocene regressive sequence and the Plio-Pleistocene regressive sequence [5-6].

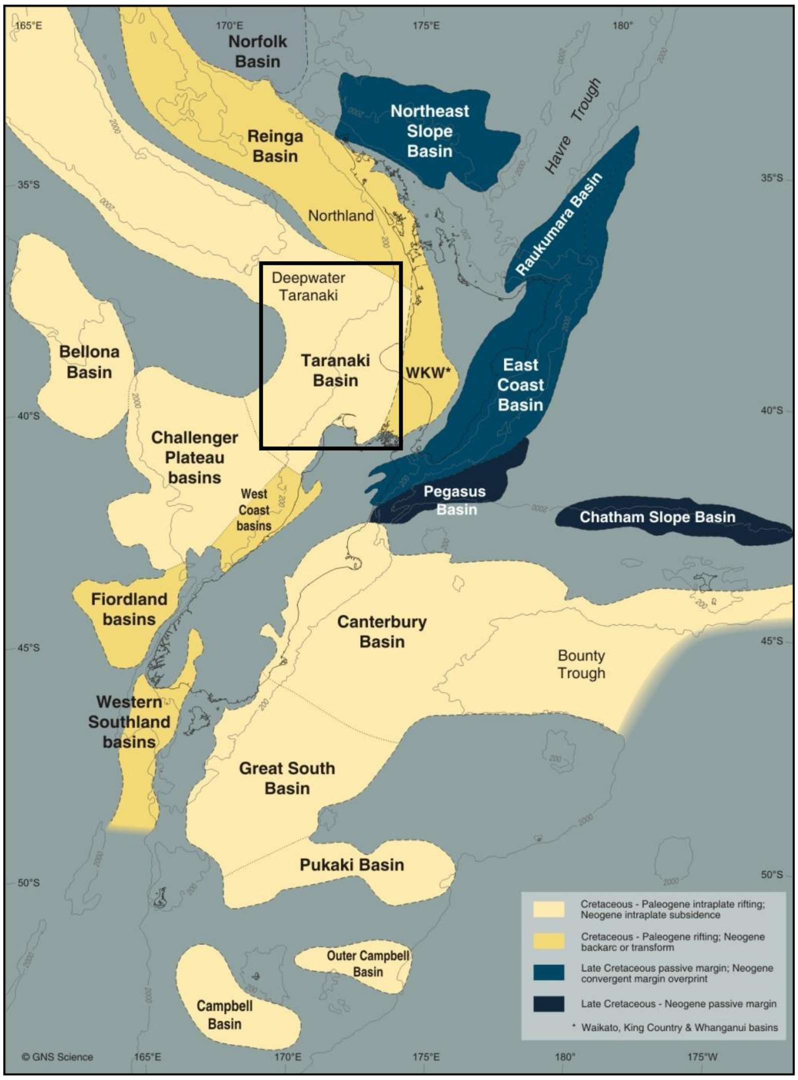

Figure 1. *Geological map of Taranaki Basin [7]*

Volume 66 (2020), No. 2
pp. 95–116, ISSN 1802-5420
DOI 10.35180/gse-2020-0035

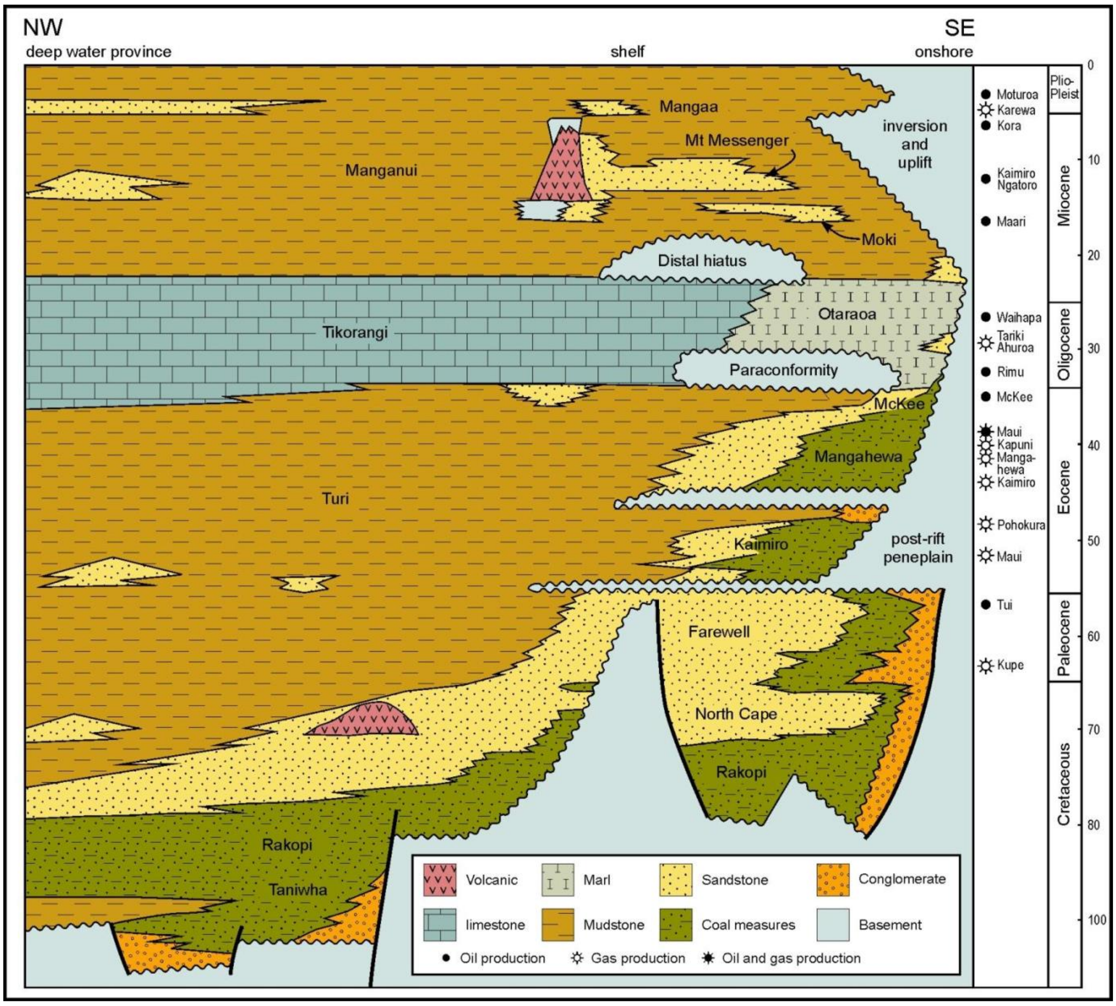

Figure 2. *Generalized stratigraphy of Taranaki Basin [7]*

3 MATERIALS AND METHODS

The seismic data set line TRV-434, acquired in the West coast of New Zealand's North Island in the Taranaki Basin by Norpac International for New Zealand Oil and Gas (NZOG) by crew No. 503 in January 1986, were used for this study. The seismic line ran across the Taranaki Fault which is a basement overthrust that formed the eastern boundary of the Taranaki Basin. The seismic line has a length of 22.7 km along 090 degrees shooting direction. The marine acquisition was carried out with Airgun as the source type and hydrophones in streamer cable as the receiver. The first shot point occurred at 101 and the last shot point at 975 with the source firing interval of 25 m firing at a water depth of 6 m. The streamer was towed at 13 m below sea level and has a total of 120 groups at 25 m group interval. The near offset and far offsets were situated at 258 m and 3233 m, respectively. The acquired data were originally de-multiplexed, trace edited, resampled and converted from SEGD to SEGY using a sampling interval of 4 ms and a high cut anti alias filter of 70–80 Hz applied to prevent aliasing during data sampling.

Data reprocessing operations commenced with data pre-processing and subsequently, the actual processing operations. The pre-processing operations include data Quality Check (QC), geometry set up, elimination of first arrivals, True Amplitude Recovery, Attenuation of Swell Noise and other unwanted high amplitude signals, Brute stack and CDP sorting. The processing operations on the other hand include Predictive deconvolution, Normal Moveout (NMO) correction, Stacking, data filtering, Velocity Analysis and Migration.

Volume 66 (2020), No. 2
pp. 95–116, ISSN 1802-5420
DOI 10.35180/gse-2020-0035

3.1. Geometry set up

Geometry information, such as location of seismic survey, shot points and seismic interval, offset distances, and other information relating to the acquisition of the regional 2D marine seismic data, usually recorded in the seismic record header were used to set up the geometry of the data and thus configured so that all traces become properly represented as acquired in space. The geometry setup ensures global configuration and enables the data appear appropriately in a format that can easily be handled by the processing software. Table 1 presents the geometry set up parameter showing the shot and receiver station intervals, sail azimuth as well as the source and receiver (streamers) depths.

Table 1. *Geometry set up and the Marine 2D Geometry parameters for Taranaki 2D marine seismic data*

Geometry Set up		Marine 2D Geometry	
Receivers Station Interval	25 m	Near Channel	1
Source Station Interval	50 m	Far Channel	119
Sail Azimuth	10°	Chan Increment	1
Source Depth	6 m	Minimum Offset	200 m
Receiver Depth	11 m	Group Interval	25 m
		No. of Shot	125
		First Shot Station	1
		Shot Station No. Interval	1
		Shot Interval	50 m

After succesful geometry set up, data quality check (QC) was performed using the ProMax DB tools to confirm if the geometry set up was appropriate as well as accertain that the recorded signals contain the right frequency bandwith required for high resolution. Amplitude check examines the amplitude record to detect faulty recording from any of the channels.

3.2. Noise Attenuation

Noise attenuation was carried out to improve the signal (desired information) to noise (everything else) ratio (S/N) of the data. This was done to suppress noise to the barest minimum, while consolidating the desired signals. Three (3) main noise types which include direct arrival, refraction and swell noise were identified on the shot gather display of the Taranaki 2D marine seismic data. Top mute tool was employed to cut off all traces having linear geometry, above the trace corresponding to the first desired primary response which normally presents hyperbolic reflection geometry, which in the case of Taranaki 2D marine data is the sea bottom reflection.

3.3. Swell Noise Attenuation

Swell noise, a high amplitude low frequency noise usually associated with feathering effect during data acquisition exercise, was identified on the shot gather displayed as linear vertical signals running through the display. Swell noise due to the distinct low frequency (2–15 Hz) was usually removed in the past simply using low cut filter to cut off the frequency range corresponding to swell noise. However, the filter also cuts off the low frequency components of the seismic data, particularly since the noise is embeded within the low frequency component of seismic signal, thereby narrowing the seismic frequency's bandwidth. This is known to greatly reduce seismic resolution, since data resolution directly relates to the broadness of the frequency bandwidth incoporatng both the low and high frequency components of the seismic data.

This study adopts a technique which eleminates undesired swell noise without narrowing the frequency bandwith by preserving the the low frequency component of the seismic signals. Attenuation was carried out in the Frequency (F) – wavenumber (K) domain because in the time domain the swell noise is deeply embeded in the signal and it is somehow difficult to design a distinct time gate for easy attenuation. Other noise types within the Taranaki 2D marine data, especially, linear noise, were subsequently removed by the application of the Radon filter which modelled the noise in the data and then substracted the modeled noise signal from the data in the frequency domain.

Volume 66 (2020), No. 2
pp. 95–116, ISSN 1802-5420
DOI 10.35180/gse-2020-0035

3.4. Predictive Deconvolution for Multiple Attenuation

Deconvolution, a processing operation commonly employed to effectively remove source wavelet effect and attenuate reverberation, short period multiple and ghosts associated with marine seismic data, was employed to improve the quality of the Taranaki 2D marine seismic data [8]. Predictive deconvolution which is apt at predicting the occurrence of periodic multiples and attenuates same by convolving it with the inverse of the source wavelet was used. This technique has been found to be very effective in identifying and removing short period multiples, especially those with constant periodicity that reoccur at specific time interval after the primary reflections. Autocorrelation, a measure of the degree of similarity between same trace over a specified time window was applied to obtain information used to design the deconvolution operator employed to define the zero lag which is the gap required to define the gap length of the DECON OPERATOR.

3.5. Velocity Analysis

Velocity analysis is a very important step in seismic data processing, usually employed to transform Two Way travel Time (TWT) seismic data into a depth calibrated reflection. Accurate velocity information is essential to flatten reflection gather for accurate NMO correction, carry out Common Mid Point (CMP) stacking and for migrating the dipping reflection events to their appropriate positions in time and space, so as to better image the subsurface. Velocity analysis was carried out on noise filtered, deconvolved and CMP stacked regional Taranaki 2D marine seismic data using brute stack velocity as the starting velocity. Velocity semblance picking panel was then used to improve accuracy, velocity range of 1400 to 5000 ms was chosen to represents the minimum and maximum semblance velocity value. The range was chosen to capture both the water velocity (this is required to map the water bottom) as well as accommodate likely high velocity formations, such as chalk that may be present within the sampled part of the basin. A lower velocity than that of the primary (e.g. multiples) will cause the gather to curve upward (overcorrection), while a higher velocity will cause the CMP gather to curve downward (undercorrection). This process was done iteratively until a near perfect velocity was picked for a particular interval. The velocities were picked at fearly wide interval to guide against error of overblown velocity which increases as the interval get significantly small [9].

The picked velocities were converted into interval velocity using Dix [10] equation (Equation 1) transform tool and the interval velocities were interpolated using linear interpolation within the various picked gather for the whole data record in order to generate isovelocity map of the Taranaki 2D marine seismic data.

$$V_{int}^2 = \frac{(V_{rms,2}^2 - t_2) - (V_{rms,1}^2 - t_1)}{t_2 - t_1} \qquad (1)$$

3.6. Normal Moveout (NMO) Correction and Angle Mute

Normal Moveout correction, which takes care of variation (increase) in reflection of arrival times due to an increase in offset distances, was applied to the Taranaki 2D marine seismic data in order to correct the reflection times of all traces relative to a zero offset acquisition geometry. The correction algorithm transforms the hyperbolic geometry of the CMP gather using the Root Mean Square (RMS) velocity to a linear (flat) gather, which brings the traces to the same datum by collapsing all traces to zero offset. This was achieved by applying a linear operator which uses a non uniform axis-streching to stretch the time axis so that all the seismograms appear like zero offset seismograms. The travel time curve of reflections for different offsets is based on the mathematical relation presented below (Equation 2).

$$t^2 = t_0^2 + \frac{x^2}{V_{stack}^2} \qquad (2)$$

NMO correction can therefore be applied using Equation 3:

$$\Delta t = t_0 - t(x) \qquad (3)$$

Volume 66 (2020), No. 2
pp. 95–116, ISSN 1802-5420
DOI 10.35180/gse-2020-0035

where

$$t(x) = (t_0^2 + \frac{x^2}{V_{stack}^2})^{\frac{1}{2}} \qquad (4)$$

However, due to the fact that the stacking velocity increases with depth and the NMO correction for the far offsets introduces NMO stretching, where far offset traces are overstretched and distorted. Thus, there is a need to mute the stretched and distorted traces, otherwise, error will be introduced to the data. Angle mute was, therefore, applied to cut off the stretched out data in order to increase or at best maintain the S/N ratio. Thirty, forty and fifty (30°, 40°, 50°) degrees mute filter were applied to get rid of the stretched out parts of the data.

3.7. CMP Stacking

All the NMO corrected reflection events corresponding to the same Common Mid Points (CMP) were extracted and sorted, the resultant data were thereafter summed together in a seismic data processing operation known as CMP stacking. This transforms the field recordings from seismic survey into a pseudo-cross-sectional image of the subsurface [11]. This involves adding all traces (redundant) corresponding to the same CMP together to form a super trace. This process combines the strength of individual traces by building up consistent signals, while eliminating non-consistent (periodic unwanted signals) ones. The NMO velocity which best flattens the gather, especially at near offset, was used as the stacking velocity for stacking.

3.8. Amplitude Recovery

Post stack amplitude recovery was performed on the marine seismic data to correct for the loss in signal amplitude (in decibel) associated with spherical divergence, wave energy attenuation as the wave travels through the subsurface and splitting of energy at seismic acoustic interfaces [12]. Waves reflected from deeper reflectors suffer most amplitude reduction, especially due to geometric divergence which varies with the inverse of the square of the distance travelled. The usual method employed to keep all reflections within the dynamic range of the recording instrument was to introduce a kind of linear field gain. True amplitude recovery, therefore, attempts to remove the field gain and add a smooth gain that compensates for the effects of signal strength attenuation as it travels within the subsurface and across the interfaces. The Taranaki 2D marine seismic data were subjected to smooth amplitude recovery at 2, 4 and 6 dB to enhance deeper reflections.

3.9. Time Variant Bandpass Filtering

Time variant bandpass filtering operation was further applied to the data to remove other unwanted signals that were still embeded in the data after several processing operations, with the aim to further increase the S/N ratio. This is particularly essential before migrating the data because the migration operation is very sensitive to noise and it is best to keep noise level at the barest minimum for effective data migration. The bandpass operation was carried out in frequency domain using Ormsby-bandpass filters. The idea behind the time variant bandpass filtering operation is that knowing the frequency range of the seismic data, it will be possible to design a gate that will keep out other data outside the defined frequency band. However, since the frequency of the seismic data can also be calibrated based on time of arrival, then instead of a single pass filter, different frequency filters can be designed and applied at different time gate based on arrival times. This method has been found to be effective for removing noise having close frequency range to that of the seismic signal as well as for separating weak signals embedded in noise. The following time variant filters (2-4-8-12; 2-8-18-22; top cut filters (2-4-70-90; 2-4-60-80; 2-4-50-70; 2-4-40-60 & 2-4-30-50) were designed and applied to the Taranaki 2D marine seismic data. Table 2 presents the designed frequency bands and the time gate to which they were applied.

Volume 66 (2020), No. 2
pp. 95–116, ISSN 1802-5420
DOI 10.35180/gse-2020-0035

Table 2. *Bandpass frequency and the time gate applied*

High cut frequency (Hz)	60–80	50–70	40–60	30–50
Application Time (secs.)	0–1	1–2	2.5–4	4.5–6.2

3.10. Post-Stack Time Migration

Migration was the last processing operation carried out on the Taranaki regional 2D marine seismic data. Different types of migration algorithms were tested in order to verify and adopt the approach with the best solution. The idea is that different migration algorithms work best under different conditions and some have strength handling some special complexities than others. Migration of seismic data is necessary to move the dipping reflection events to their appropriate positions in time and space. This is particularly necessary because the data acquisition process and indeed recording system assumes a flat reflector, thus based on the Snell's law records all reflection arrivals at a depth point (CDP) that is located half way between the source and the receiver (offset), that is at Common Mid-Point. However, because the earth reflectors are rarely flat, it means that reflections from dipping events are wrongly recorded since Snell's law breaks down for dipping beds [12, 13]. Unmigrated seismic section, therefore, has some ambiguities that impeed the ability to properly image the subsurface, some of which include the fact that events are not properly represented in time and in space, having an apparent dip instead of the true dip. Synclines on unmigrated seismic section appear narrower and sometimes with bow-tie, anticlines appear broader and a point is spread out as diffraction, creating diffraction curves which often cross each other. Generally, the resolution of an unmigrated seismic record is poor and sometimes having partial smearing [12]. Migration algorithm corrects all the short comings so that the primary events represent real geologic events which are distinct from other seismic geological responses.

Kirchhoff migration, which migrates dipping events by summation the diffraction curves over a semicircle, was the first migration method tested on the seismic data. This migration method has the strength of preserving the amplitude and the phase of the data after migration [14]. It also has the flexibility that it can be applied both on pre and post stack data as well as be applied in time and depth domain [15]. The migration process began with the generation of synthetic for swing test at 45°, 65° and 90° swing tests. The picked velocities during velocity analysis were used as the migrating velocity. The migration was carried out at CDP interval of 12.5 m and a maximum frequency to migrate was set to 60 Hz, while the migration maximum dips were set to 45° and 75° respectively. Finite Difference (FD) migration, which is based on the wave equation in the time domain, phase shift migration which assumes constant lateral but varying vertical velocity as well as the Stolt migration algorithm that assumes constant velocity, were also applied to generate solutions that best image the subsurface geology.

3.11. Pre-Stack Time Migration

Prestack Kirchhoff Time Migration (PreSTM) which is an advanced migration technique over PSTM techniques was also applied, especially because of its strength in resolving complex subsurface geology and structures which could present steep dips up to 90° and lateral variation in velocity. This is particularly necessary to resolve complex subsurface geology and structures that characterised the Taranaki Basin. The main objective of prestack migration is to transform common shot offset gather into Common Image Point (CIP). The first step carried out involves backing off the NMO and sort data to a common shot offset plane. The unstacked data in the common offset plane were subsequetly migrated using the PreSTM algorithm. The postack migration velocity was used as the starting velocity because the PreSTM requires more accurate velocity.

4 RESULTS AND DISCUSSIONS

The results obtained by the application of various recent seismic data processing techniques applied to reprocess the regional Taranaki 2D marine seismic data (TRV-434**)** to improve the quality of the subsurface image derivable from the seismic data are presented in this section. The data reprocessing operation commenced with geometry

Volume 66 (2020), No. 2
pp. 95–116, ISSN 1802-5420
DOI 10.35180/gse-2020-0035

setting for appropriate configuration of the seismic data so that all traces were properly represented in conformity with the acquisition design. A plot of the station geometry presents the CDP fold geometry (Figure 3) which indicates the lead in and the lead out sections as well as the full fold (60) section of the data.

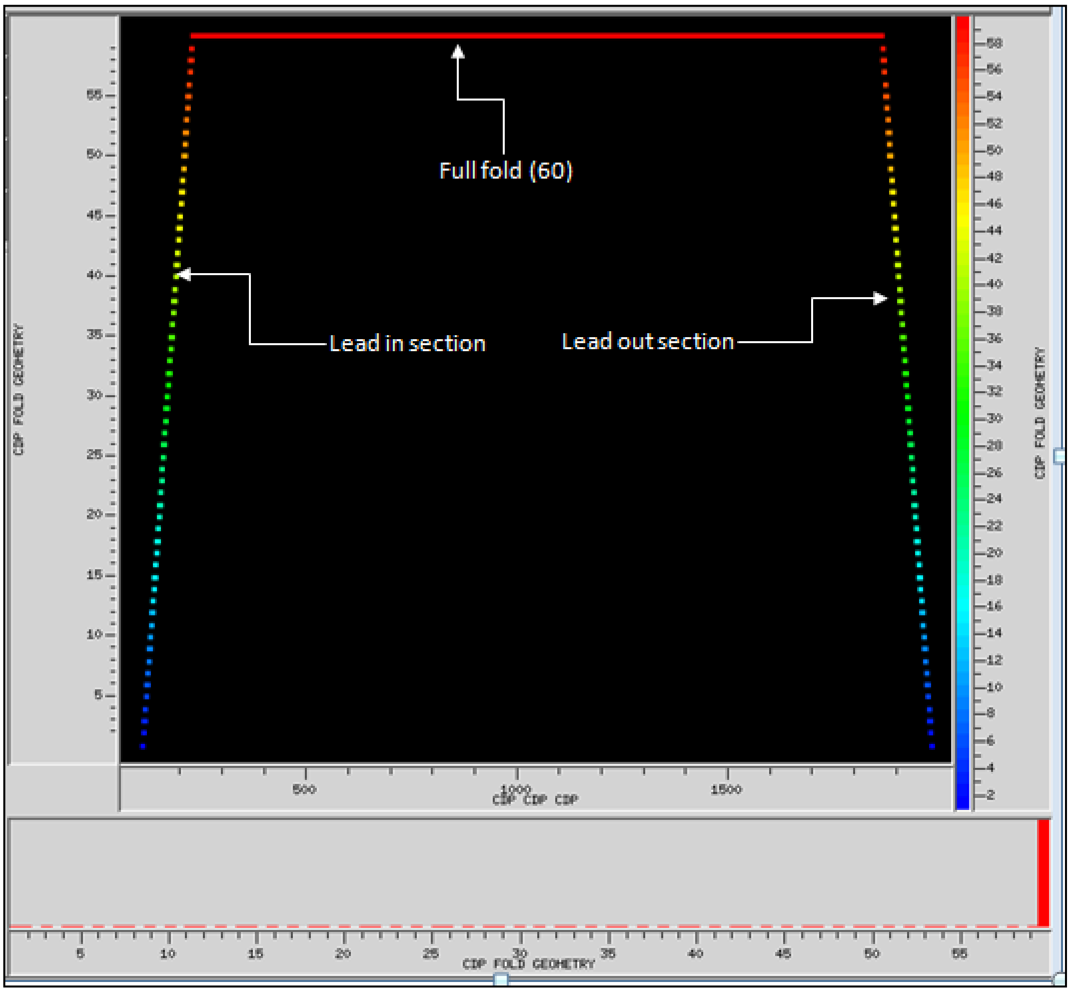

Figure 3. *CDP fold geometry showing the lead-in, full fold and the lead-out section*

Data QC of appropriately set up seismic data identified and ensured that noisy data, especially those from faulty channels, were eliminated to increase the S/N ratio. Figure 4 presents the amplitude record of all the sampled channels showing those channels having anomalously high amplitude, especially at channels 55 and 92 as well as near source channels (115 to 120), caused by their proximity to the energy source. Additional data QC operation which examined the frequency spectrum indicates that almost all the necessary frequency bands were preserved.

Volume 66 (2020), No. 2
pp. 95–116, ISSN 1802-5420
DOI 10.35180/gse-2020-0035

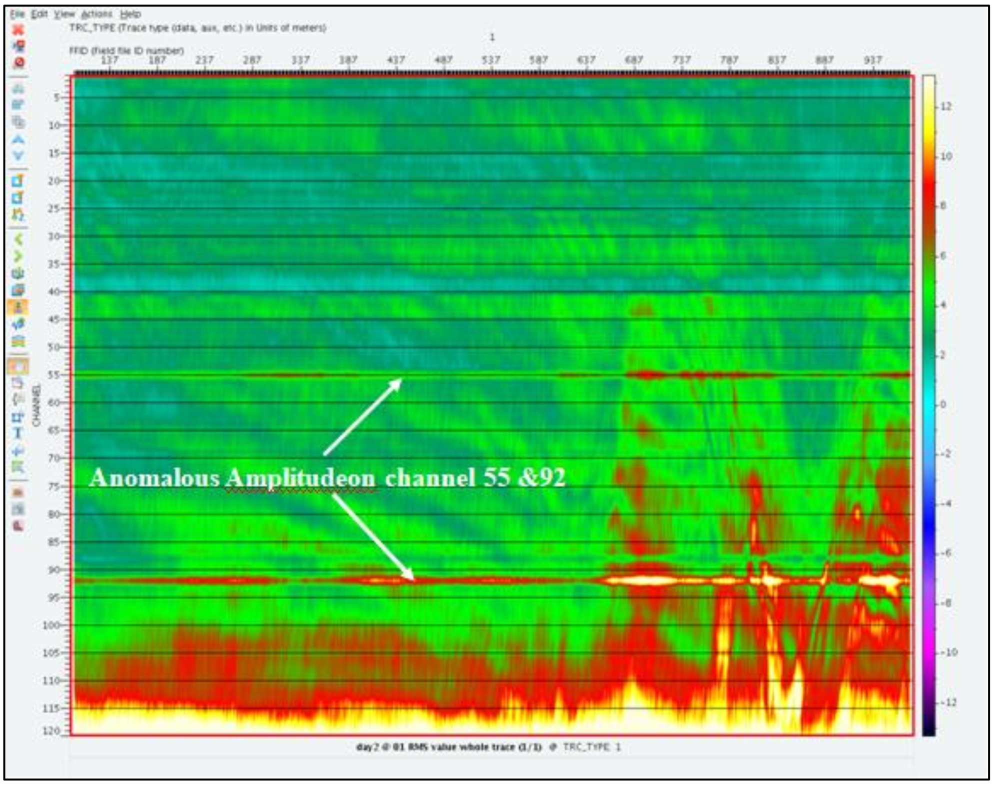

Figure 4. *Amplitude plot for all channels showing channels with anomalous amplitude signals*

Muting of the first arrival using the top mute cut off was the first pre-processing operation carried out. Figure 5 is a raw shot gather of the Taranaki marine seismic data showing some unwanted (direct arrival, refraction and swell noise) reflection events, while Figure 6 presents the resultant top muted seismic data after the application of top mute cut off tool to remove all the linear geometry unwanted reflections.

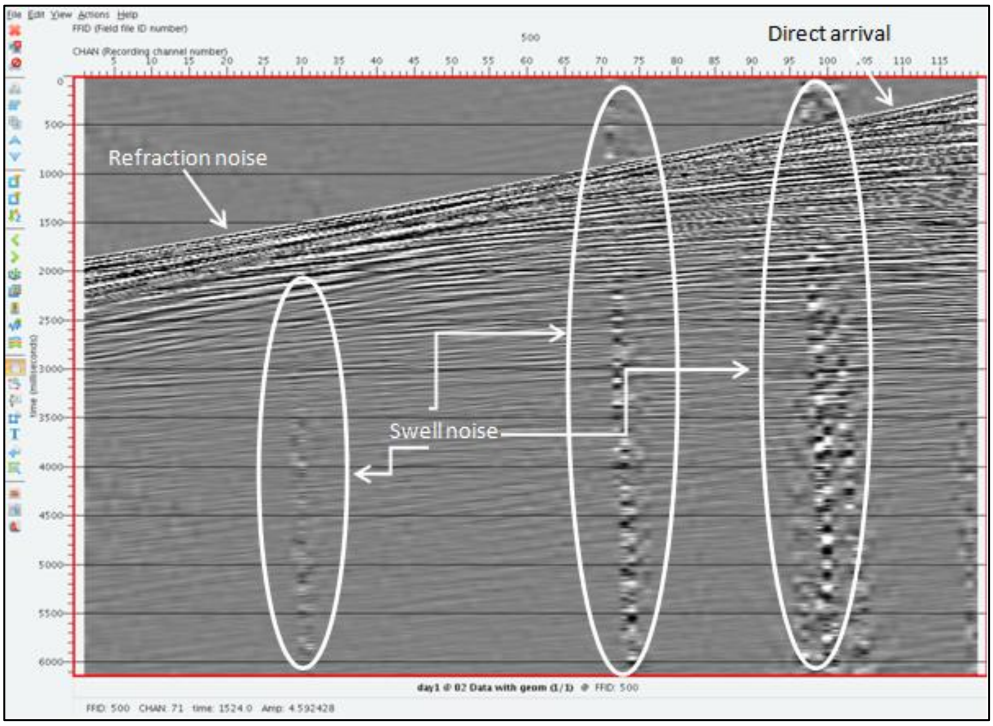

Figure 5. *Some unwanted seismic signal energies*

Volume 66 (2020), No. 2
pp. 95–116, ISSN 1802-5420
DOI 10.35180/gse-2020-0035

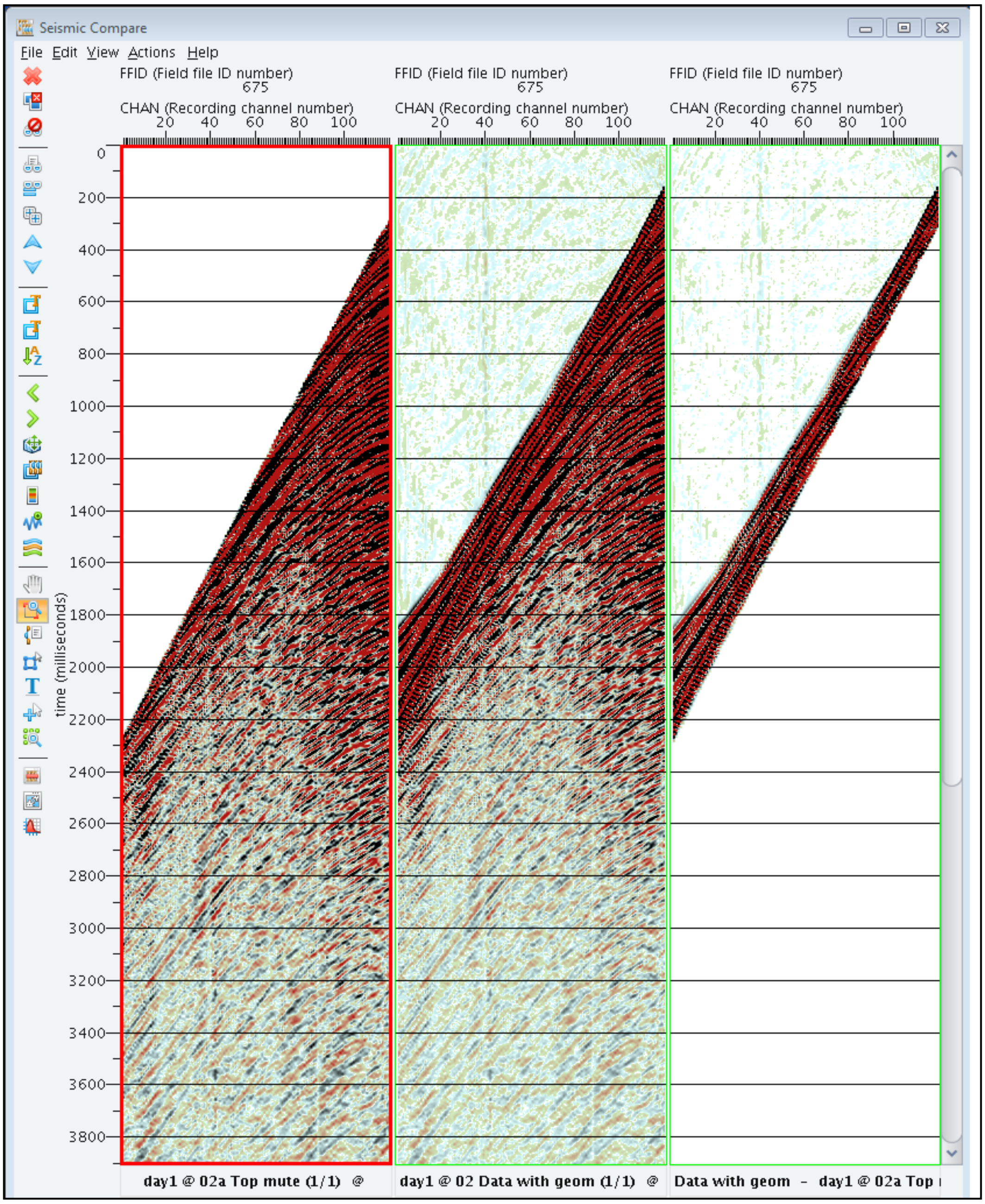

Figure 6. *Top muted, raw and muted out unwanted reflections by the application of top mute filter*

4.1. Autocorrelation

The autocorrelation of Taranaki seismic traces carried out to generate information required to design effective predictive DECON OPERATOR is presented in Figure 7 which indicates the water bottom reflection, zero lag crossing, ghost reflection and the water bottom multiple with their respective TWT(s). The figure also shows that the water bottom multiple dips from east to west as the water bottom gets shallower from right to left.

Volume 66 (2020), No. 2
pp. 95–116, ISSN 1802-5420
DOI 10.35180/gse-2020-0035

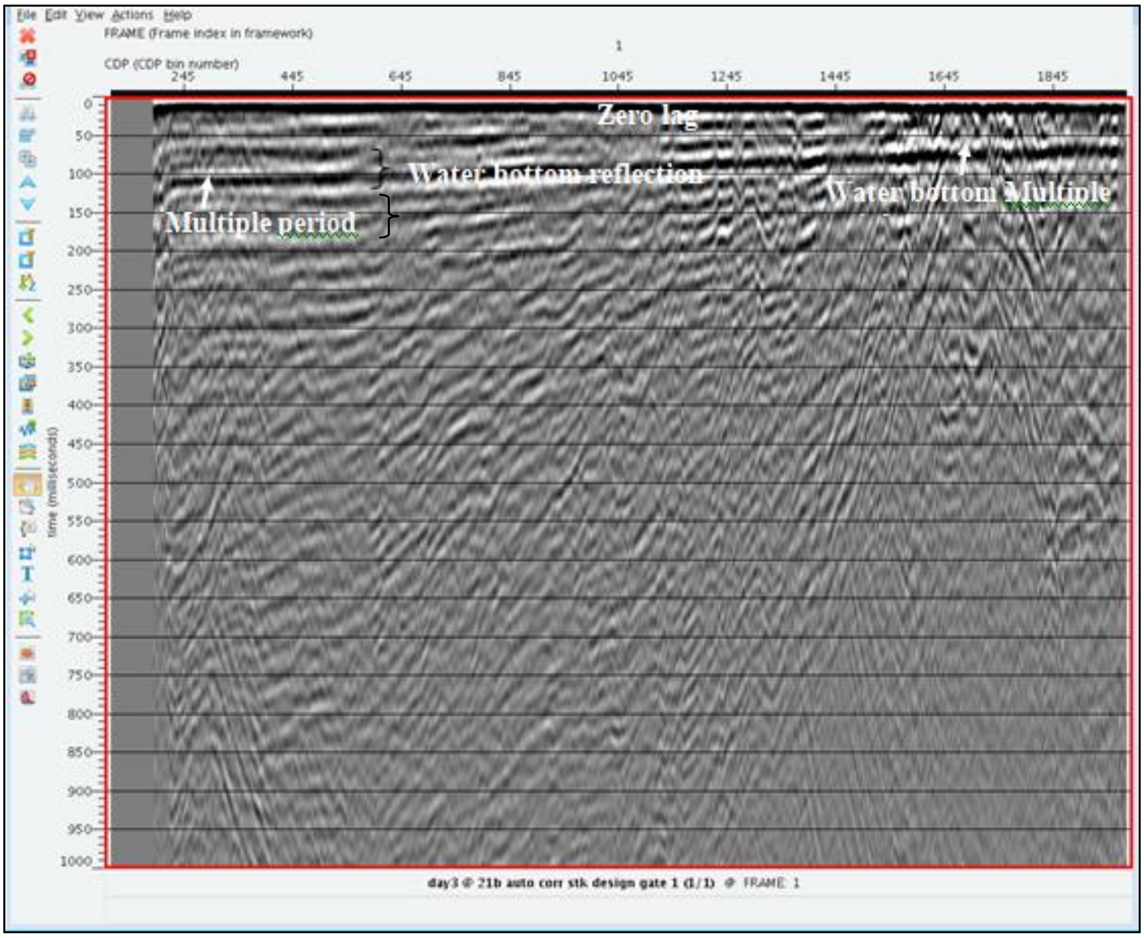

Figure 7. *Autocorrelation of Taranaki 2D marine seismic data showing zero phase lag, water bottom reflection and multiples*

The autocorrelation output indicates the streamer ghost is located at 17 ms, very close to the water bottom arrival, while the first water bottom multiple occured at 90 ms (Figure 7). The receiver/streamer ghost, which is a reflection of the sea surface, is located at 17 ms later than the source ghost. This is because the streamer was placed at water depth of 13 m.

4.2. Predictive Deconvolution

Two parameters were defined from the autocorrelation solution, the zero lag and the gap used to define the DECON operator/ gap and length. A gap of 24 and 28 ms and operator's length of 100 and 200 ms, respectively, predicted and removed the water bottom multiple without tempariing (preserved) with the primary reflection event. A comparison after predictive deconvolution with 24 ms and 100 ms gap and length, respectively, is presented in Figure 8 which indicates the removal of the water bottom multiple observed in the undeconvolved (right panel) seismic record.

Volume 66 (2020), No. 2
pp. 95–116, ISSN 1802-5420
DOI 10.35180/gse-2020-0035

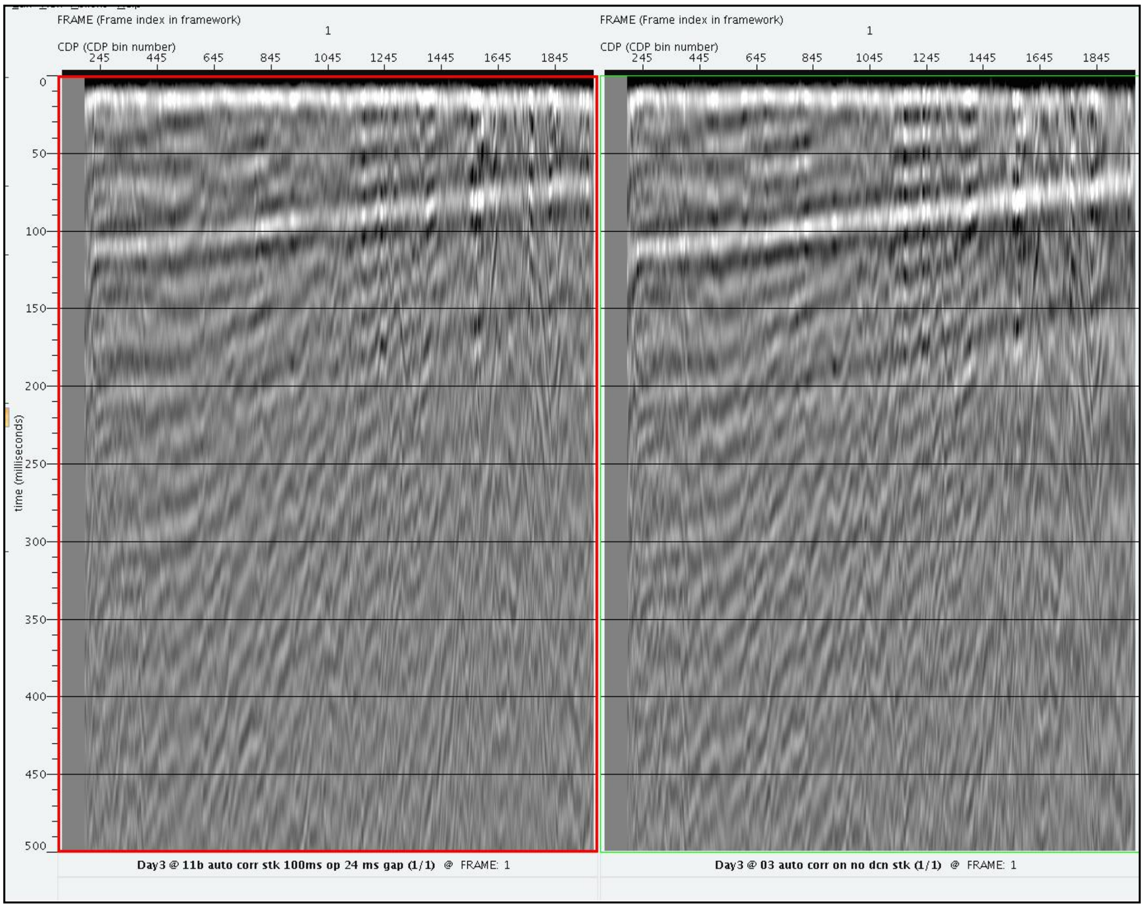

Figure 8. *Result of predictive deconvolution, showing attenuation of some multiple energies*

4.3. Velocity Analysis

The semblance pannel used for picking the correct velocity that flattens the CMP gather is presented in Figure 9 (a–c). The first column is the semblance display, the bold line is the guide function, corresponding to the brute velocity function that was used to stack the data. The measure of semblance is presented as colour variation, the higher the semlance, the higher the coherency. The second column is the super gather, while the third is the constant velocity stack at the specified interval. Velocity picking started around 300 ms to avoid the taper zone with limited data. The water velocity (1448 m/s) was the first to be picked which is a lower velocity than the reflection primaries and thus bends primary reflections upward as an effect of overcorrection (Figure 9a). The second pick corresponds to the rock velocity at the second NMO and it attempts to flatten the gather (Figure 9b). The velocities which flatten the gather at the near, mid and most part of the far offset are selected with the aid of the interactive velocity picking tool as the accurate velocity information.

Volume 66 (2020), No. 2
pp. 95–116, ISSN 1802-5420
DOI 10.35180/gse-2020-0035

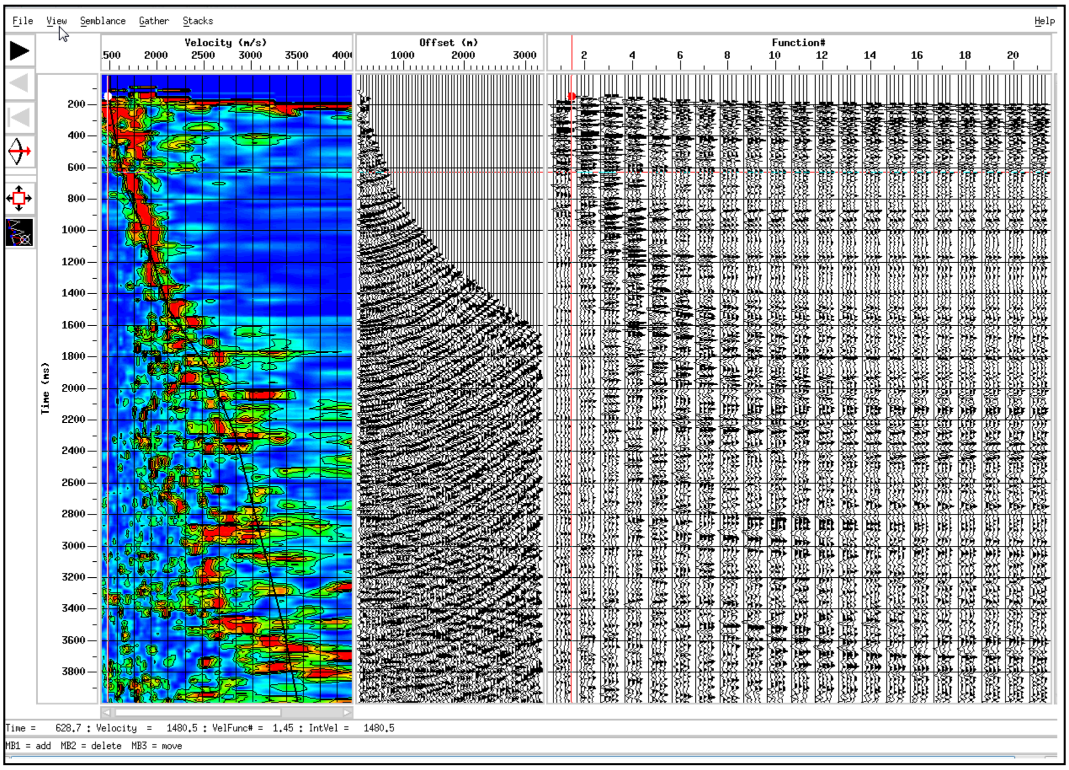

Figure 9(a). *Velocity picking panel showing bending upward gather due to velocity undercorrection from picked low velocity (water velocity)*

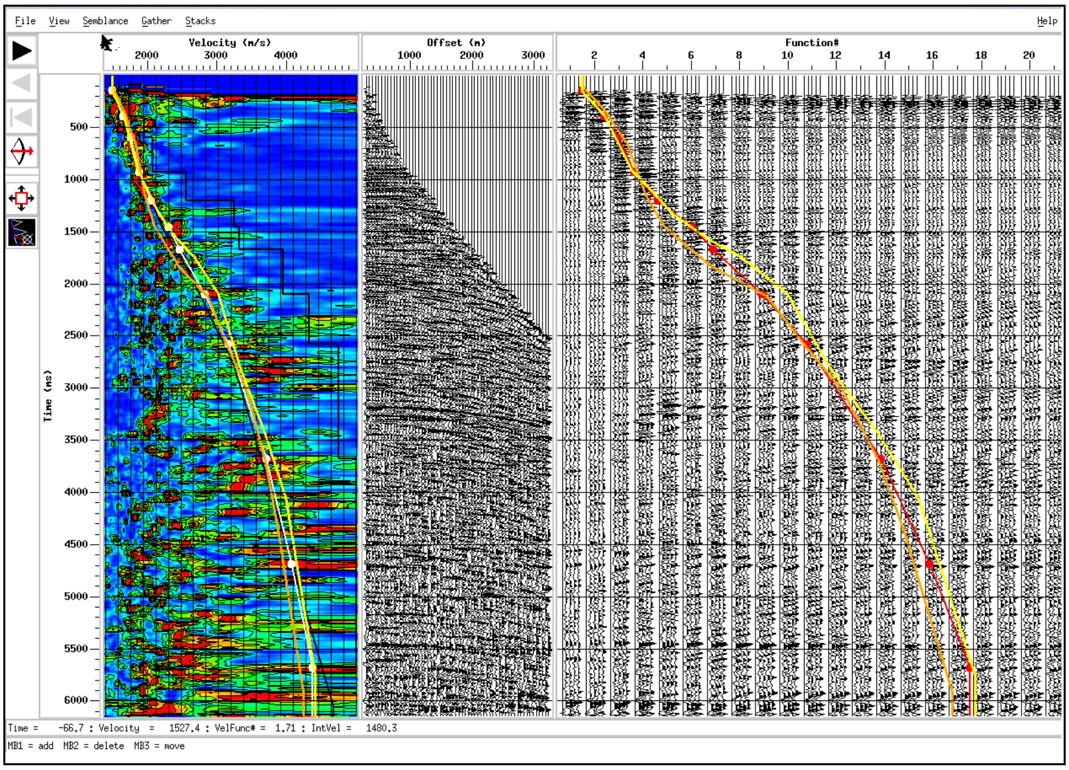

Figure 9(b). *Velocity picking panel showing the seblance panel, supergather*

Volume 66 (2020), No. 2
pp. 95–116, ISSN 1802-5420
DOI 10.35180/gse-2020-0035

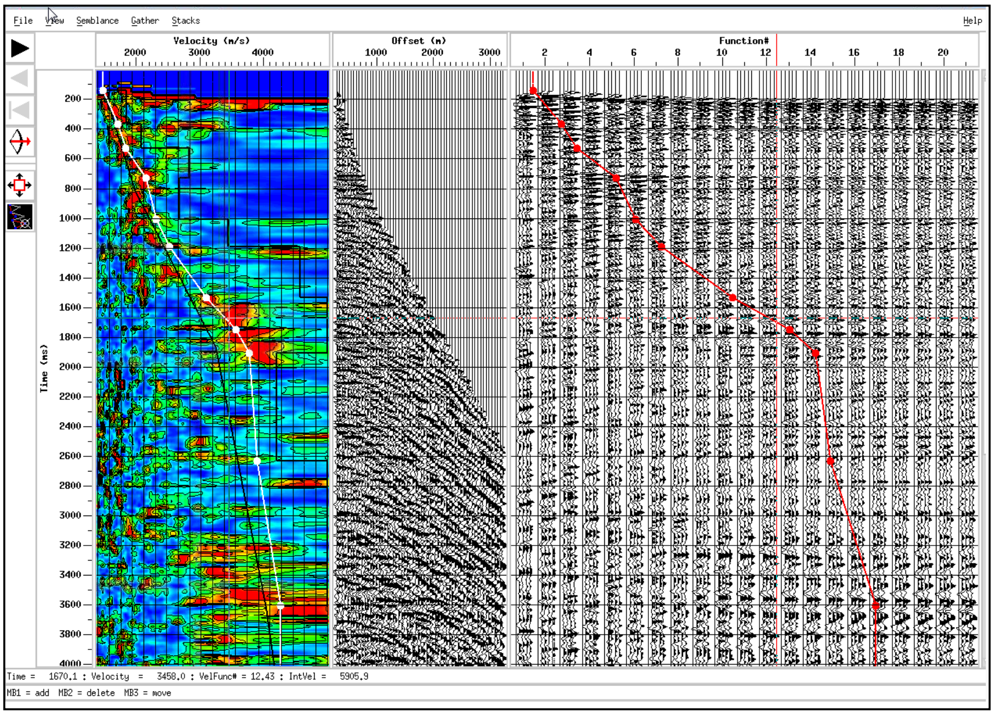

Figure 9(c). *Downward bending gather due to picking multiple (lower) velocity*

The computed and smoothened interval velocities generated by interpolating (lineaar interpolation) all the picked velocities (at 100 ms) within the various gather for the whole data record and converted to interval seismic velocity using DIX [10] relation is presented in Figure 10 as an isovelocity map of the Taranaki 2D marine seismic data. The isovelocity map indicates regions of low and high interval velocities, where the interval velocity generally increases with depth.

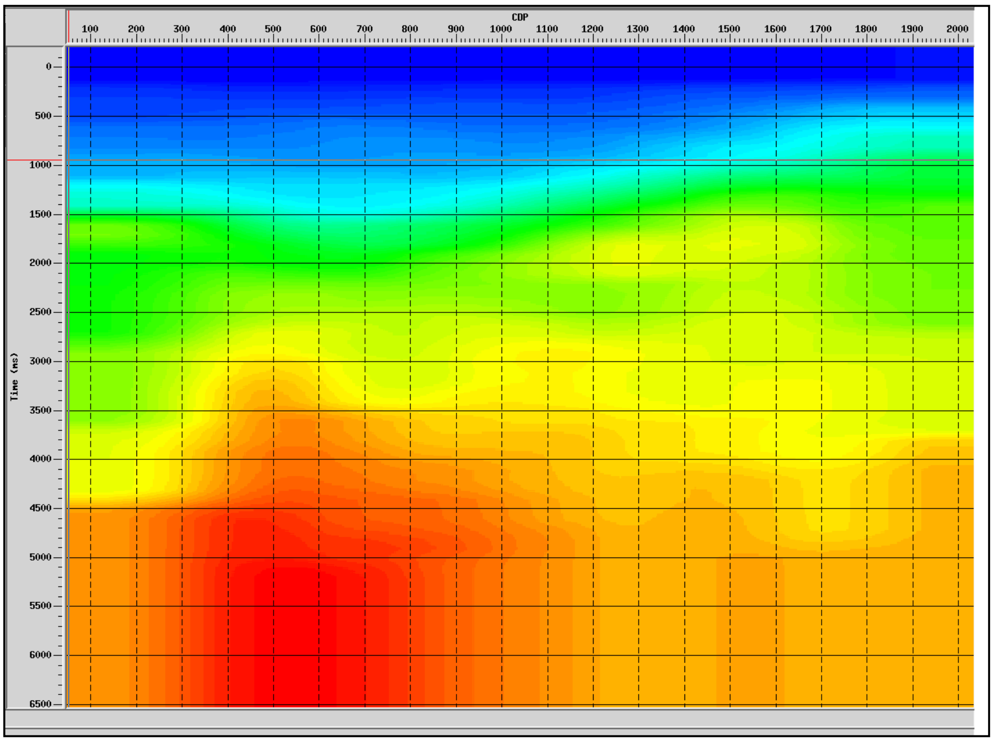

Figure 10. *Smoothened interval velocity of 2D seismic data of Taranaki*

Volume 66 (2020), No. 2
pp. 95–116, ISSN 1802-5420
DOI 10.35180/gse-2020-0035

4.4. Amplitude Recovery

The stacked section after the application of amplitude recovery gain to the Taranaki 2D marine seismic data is presented in Figure 11. A comparison of the recovered (left panel) and the unrecovered seismic image (right panel) indicates that the effect of amplitude recovery is more visible in the lower part of the section, showing that the lower reflections become better visible after the application of the gains, while reflections corresponding to the shallower part receive very little amplification. This is because the true amplitude recovery is travel time dependent; reflections from deeper reflector which have suffered more spherical divergence and attenuation for travelling longer were more gain recovered than the reflections from shallower reflectors which suffered less.

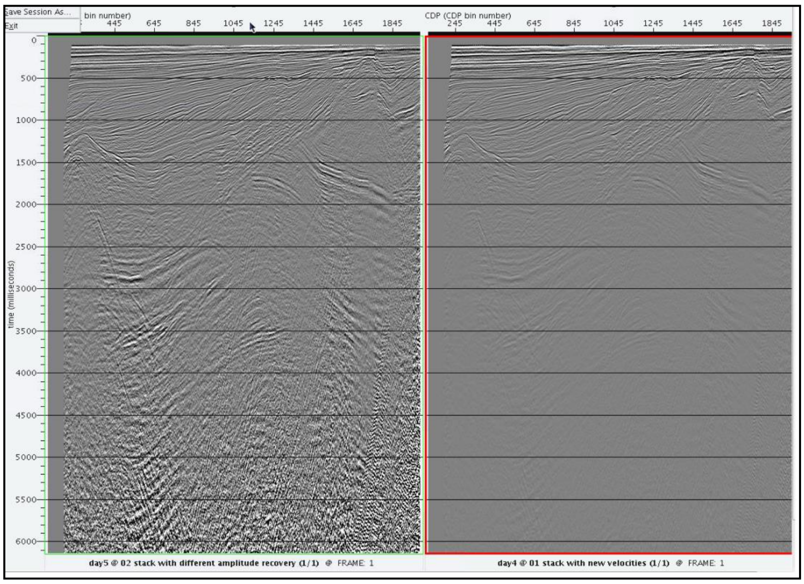

Figure 11(a). *Comparison of stacked section after true amplitude recovery*

The reflections amplification upon the application of 2 dB and 6 dB gain is presented in Figure 11(b). The 2 dB gain recovered output appear to boost all desired reflections to detectable scale, while the 6 dB (right panel) gain recovered output appeared too high, showing overamplification of signals and the noise content as well.

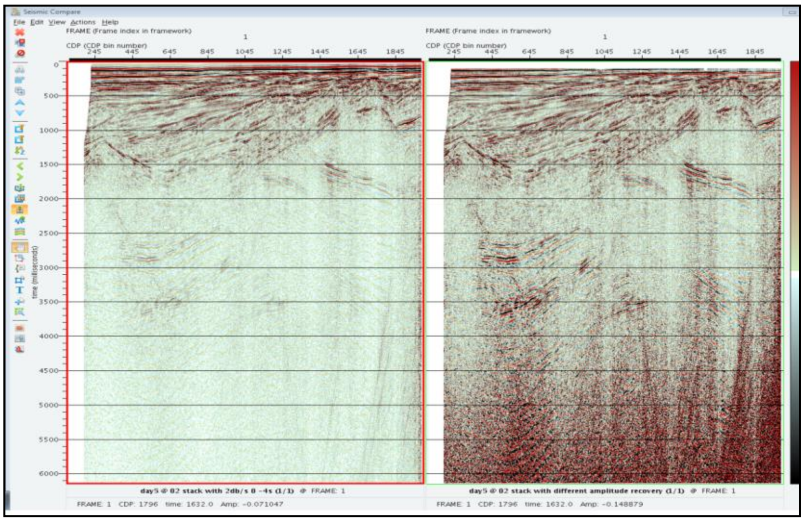

Figure 11(b). *A comparison of Amplitiude Recovery with 2 dB and 6 dB respectively*

Volume 66 (2020), No. 2
pp. 95–116, ISSN 1802-5420
DOI 10.35180/gse-2020-0035

4.5. Normal Moveout Correction and Angle Mute

Normal Moveout stretching of the far offset reflection traces after NMO correction results usually show the distorted longer offset traces. The angle mute applied cut off the stretched out and distorted traces using 30°, 40°, 50° angle mute filters successively to increase the S/N ratio. The 40° mute line (green) cuts off all traces above the mute line in order to eleminate the distorted reflection traces (Figure 12a). However, the occurrence of some poorly resolved (distorted) traces still below the 40° mute line suggest the need to apply a higher angle mute line, and hence the application of 40° and 50° angle mute filters.

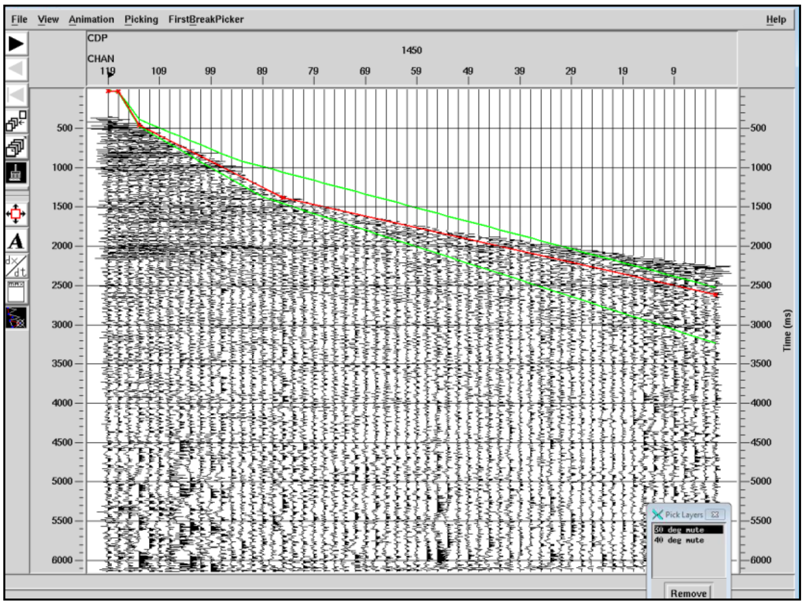

Figure 12(a). *40° and 50° angle mute filter line*

Figure 12b compared the 30° and 50° angle mute filtering output of stacked Taranaki 2D marine seismic section, which indicates an effective removal of significant proportion of the stretched and distorted traces with the 50° mute filter than the 30° mute filter. The resolution of the record obtained by the application of 50° mute filter (right panel) appeared higher than that of the 30° (left panel) with an increase in the S/N ratio.

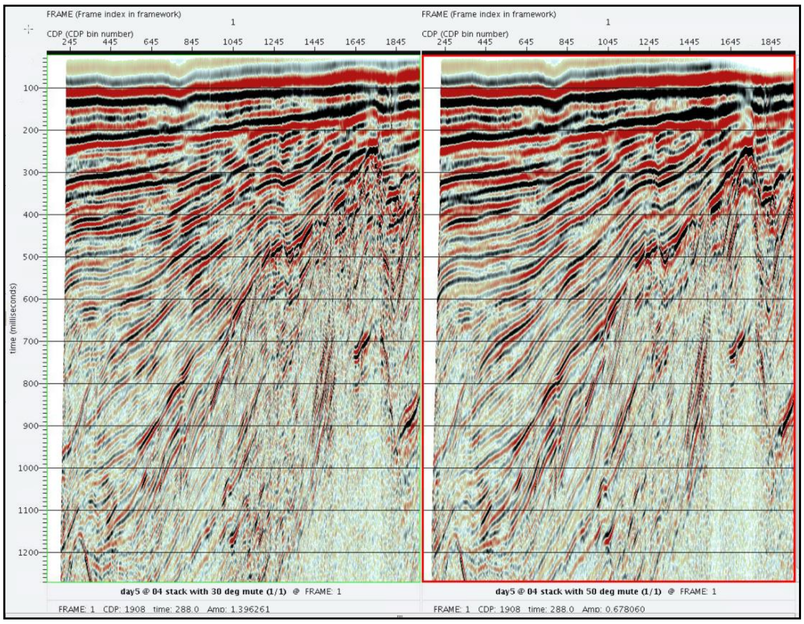

Figure 12(b). *Angle mute effect on the upper part of the section displays*

Volume 66 (2020), No. 2
pp. 95–116, ISSN 1802-5420
DOI 10.35180/gse-2020-0035

4.6. CMP Stacking

Stacked, sorted and NMO corrected traces corresponding to the same CMP is presented as CMP stacked gather of Taranaki seismic data in Figure 13 showing the relatively higher signal to noise ratio record. The figure also shows that some of the noise, especially the non-coherent energies have been collapsed and attenuated to a reasonable level.

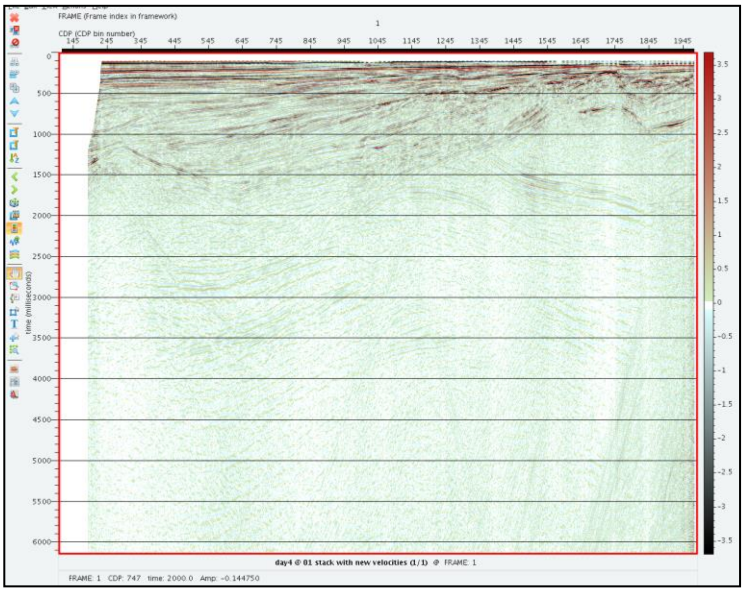

Figure 13. *Common Mid Point (CMP) stack section of Taranaki 2D marine seismic data*

4.7. Time Variant Bandpass Filtering

The application of the time variant bandpass filters at different time gates, which remove unwanted signal energies still present in the seismic data, gave different results but the geophysically plausible solutions which preserve desired signal were accepted. The resultant records after the application of the different bandpass filters are presented in Figure 14.

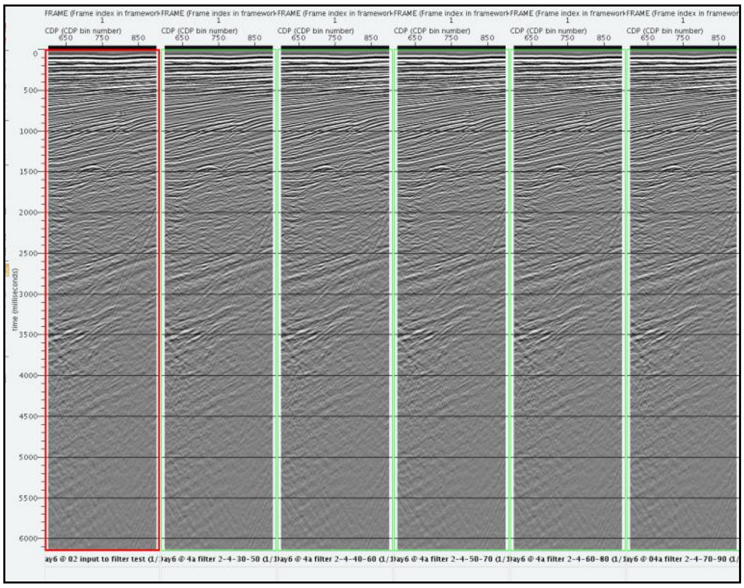

Figure 14. *Effects of application of different bandpass filters*

Volume 66 (2020), No. 2
pp. 95–116, ISSN 1802-5420
DOI 10.35180/gse-2020-0035

The difference between the unfiltered and filtered records shown in the seventh, eight and the ninth panels (Figure 15) indicates that the filtering operation is effective being able to filter out seismic energies that did not correspond to primary reflections.

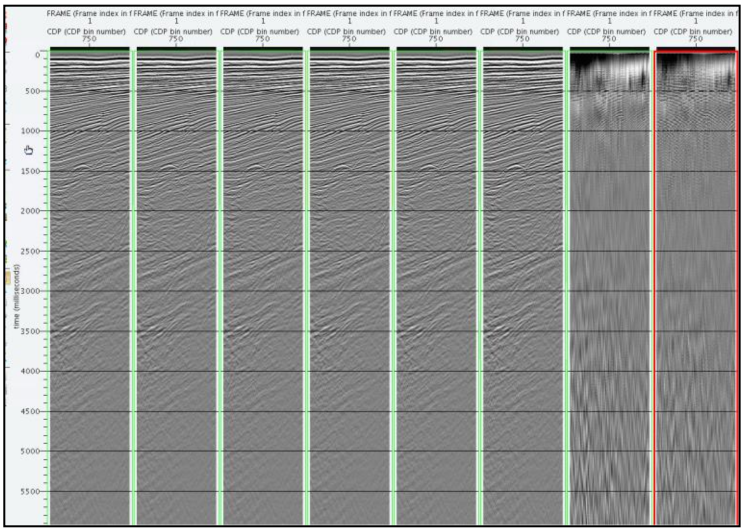

Figure 15. *Difference between the unfiltered and filtered records showing the filtered outreflection energies*

4.8. Post-stack Kirchhoff Time Migration (PSTM)

The resultant seismic record after the application of Post-stack Kirchhoff Time Migration at maximum migration angle of 45° and 75° indicate significant improvement in the resolution of the Taranaki 2D marine seismic record (Figure 16 (a & b)), especially when compared with unmigrated stack record (Figure 13). Visible improvements include the disappearance of many of the crossing events and diffraction curves visible on the un-migrated stack section. However, evidence of overcorrection, commonly referred to migration smiles, which are presented as upward bending of reflection events due to low migration velocity, become more apparent in the lower (deeper) part of the section (Figure 16 (a & b)).

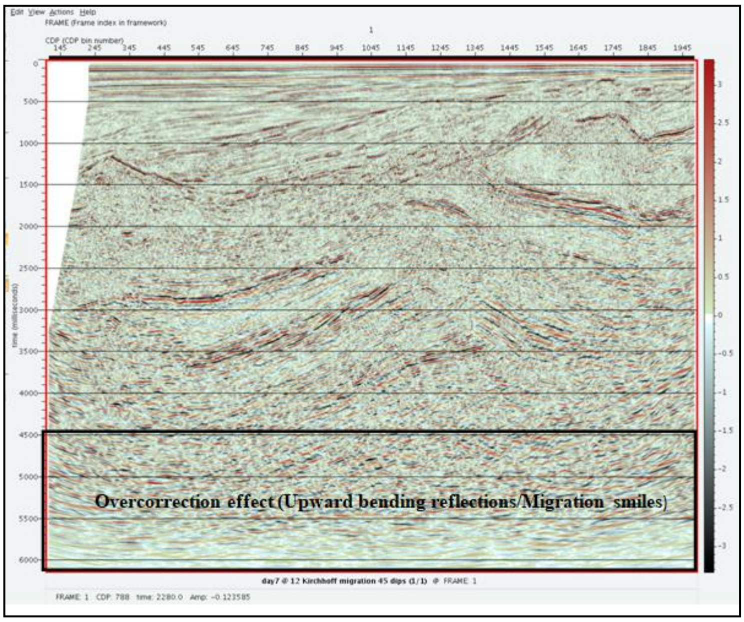

Figure 16(a). *Kirchhoff Time Migration at 45°*

Volume 66 (2020), No. 2
pp. 95–116, ISSN 1802-5420
DOI 10.35180/gse-2020-0035

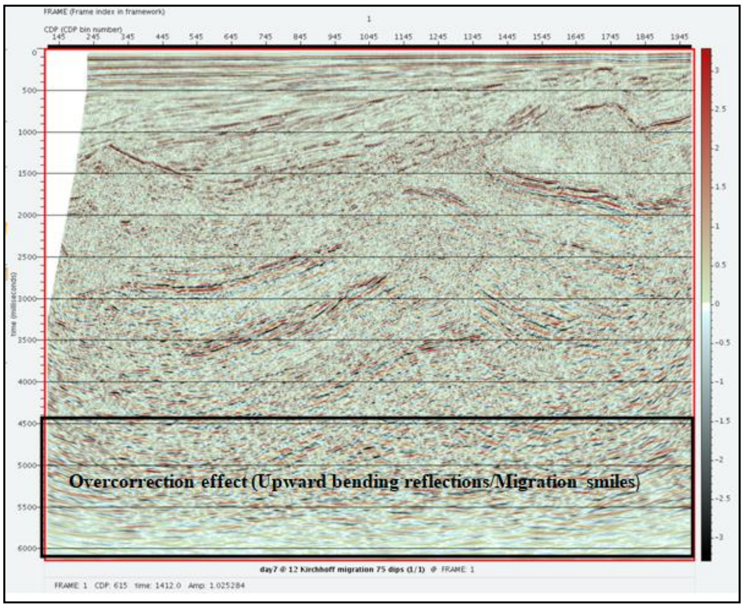

Figure 16(b). *Kirchhoff Time Migration at 75°*

Finite Difference (FD) migration, which is based on the wave equation in the time domain, phase shift migration which assumes constant lateral but varying vertical velocity, as well as the Stolt migration algorithm that assumes constant velocity were applied. A comparison of the results of the Kirchhoff Time Migration at 75° with the Phase shift migration and Stolt migration methods on the Taranaki 2D marine seismic data (Figure 17) indicate that all the three migration algorithms migrated the data relatively effectively with the disappearance of some of the diffraction curves and some of the crossing events as well. However, there are still some migration curves and the resolution of the data could be improved.

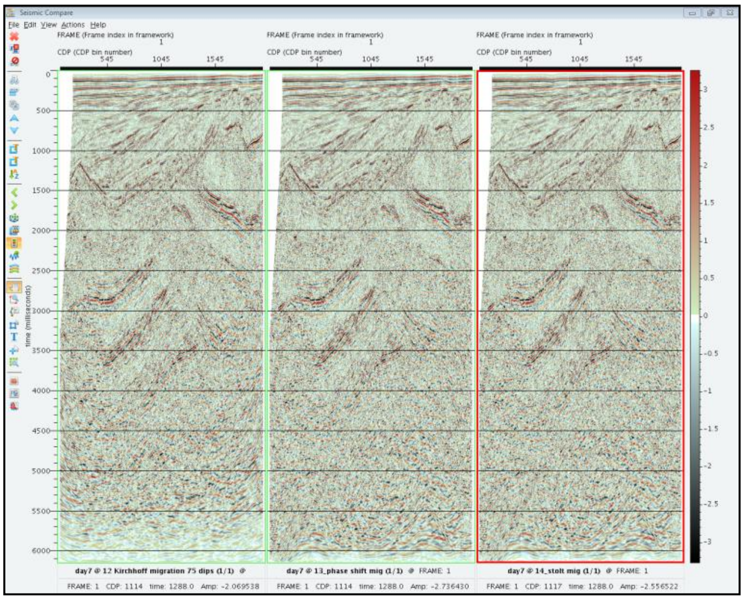

Figure 17. *Comparing the different migration results (Kirchhoff, Phase shift and Stolt)*

Volume 66 (2020), No. 2
pp. 95–116, ISSN 1802-5420
DOI 10.35180/gse-2020-0035

4.9. Pre-Stack Kirchhoff Time Migration

The satisfactory quality of pre-stack Kirchhoff time migration solution, especially its strength to handle image complexity associated with complex subsurface geology commonly presented in the form of complex velocity variation (e.g. occurrence of salt structure) and steeply dipping structures has made the pre-stack migration a migration method of choice despite the cost in terms of huge computer processing capacity and time, especially for handling numerous (prestack) data. The application of pre-stack Kirchhoff time migration algorithm introduced several improvements in the quality of the Taranaki 2D marine seismic data. This includes the dissapearance or flattenning of migration curves/smiles (migration artifacts) caused by an overcorrected deeper layer (Figure 18). Another noticed improvement is the increase in the resolution of the deeper reflections which appeared blured/unresolveable with other migration techniques, including the post-stack Kirchhoff migration.

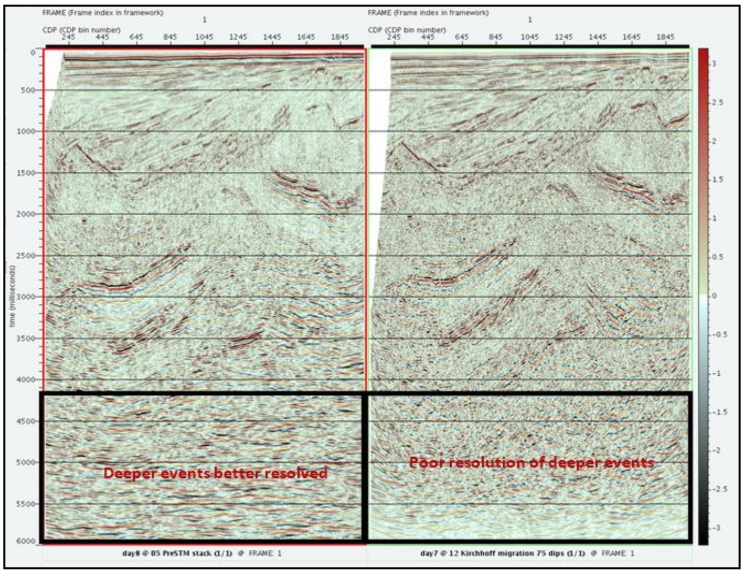

Figure 18. *Comparison between Post and Pre-stack Kirchhoff Time Migration showing better resolved deeper reflections*

In general, the newly processed, stacked migrated Taranaki 2D marine seismic records presented in Figure 19 show a lot of improvements when compared with the raw seismic data, and the initially processed Taranaki seismic data which present lower resolution with many diffraction curves.

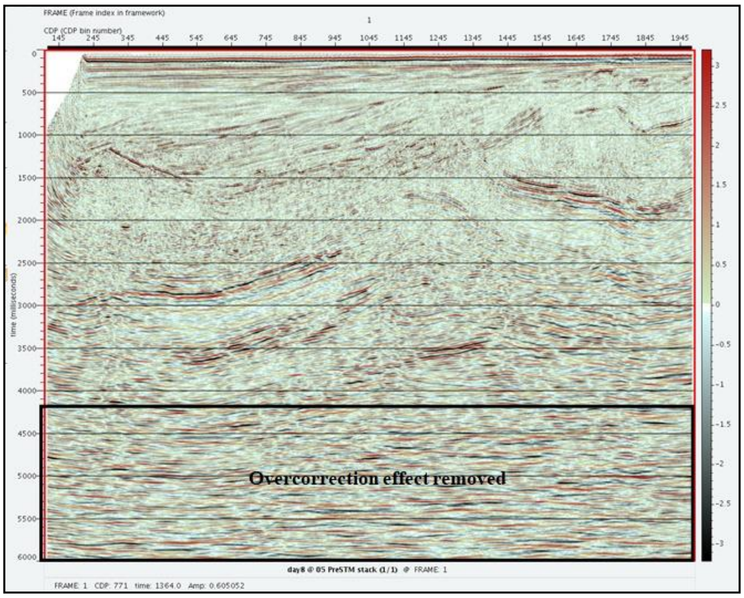

Figure 19. *Processed, migrated and stacked Taranaki 2D marine seismic section*

Volume 66 (2020), No. 2
pp. 95–116, ISSN 1802-5420
DOI 10.35180/gse-2020-0035

A very quick interpretation of the seismic section of the reprocessed, migrated and stacked Taranaki 2D marine seismic section, carried out in order to quality check the resultant seismic record, especially to ascertain the ability of the reprocessed data to accurately image the subsurface geology, is presented in Figure 20. The reprocessed seismic record presents subsurface features, such as faults as well as several folded and unfolded horizons that are consistent to the subsurface geology described by several authors [16-20], who used several information, including geologic field mapping, well information, gravity and seismic records to reconstruct the geology of the Taranaki Basin. The integrity of the reprocessing is underscored by the clear imaging of the popular back thrust antithetic Taranaki Fault as well as Top basement which have been previously identified and interpreted from the old seismic data [21].

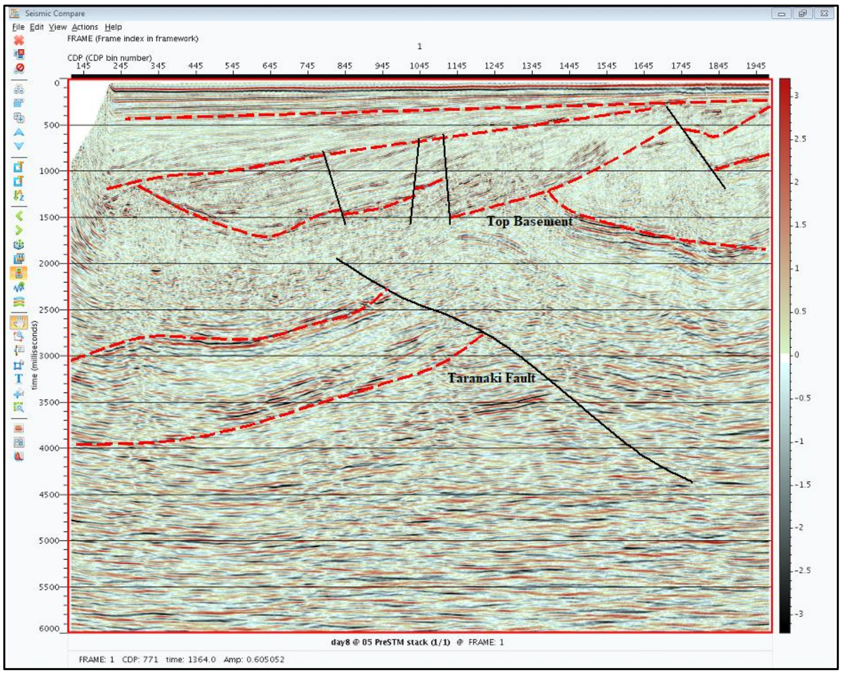

Figure 20. *Interpreted processed, migrated and stacked Taranaki 2D marine seismic section*

5 CONCLUSIONS

The data reprocessing of the regional 2D marine seismic data of part of Taranaki Basin which is the only known basin (so far) with hydrocarbon potential in New Zealand using newer processing techniques which had not been available as at the time when the data were acquired in the 1980's (1986) has yielded a better enhanced seismic record, thus providing a clearly resolved subsurface geologic information despite complex geologic structures that characterised the basin. This study demonstrates the improved quality of subsurface information derivable from reprocessing of old available seismic data using new techniques. The reprocessed 2D marine seismic data of Taranaki Basin generated valuable information useful for hydrocarbon prospect evaluation of the basin. The generated subsurface information could also help to guide the design as well as narrow the search zones to focus on using *state-of-the-arts* seismic acquisition techniques.

REFERENCES

[1] ARMSTRONG, P.A., D.S. CHAPMAN, R.H. FUNNELL, R.G. ALLIS and P.J.J. KAMP. Thermal modeling and hydrocarbon generation in an active-margin basin: Taranaki Basin, New Zealand. *AAPG Bulletin*. 1996, 80(8), pp. 216–1241. DOI: https://doi.org/10.1306/64ED8CF0-1724-11D7-8645000102C1865D

[2] ILG, B.R., S. HEMMINGS-SYKES, A. NICOL, J. BAUR, M. FOHRMANN, R. FUNNELL and M. MILNER. Normal faults and gas migration in an active plate boundary, southern Taranaki Basin, offshore New Zealand. *AAPG Bull*. 2012, 96(9), pp. 1733–1756. DOI: https://doi.org/10.1306/02011211088

[3] KNOX, G. J. Taranaki Basin, structural style and tectonic setting. *New Zealand Journal of Geology and Geophysics*. 1982, vol. 25, pp. 125–140. DOI: https://doi.org/10.1080/00288306.1982.10421405

[4] VONK, A.J. and P.J.J. KAMP. The Late Miocene Southern and Central Taranaki Inversion Phase (SCTIP) and related sequence stratigraphy and paleogeography. In: *2008 New Zealand Petroleum Conference Proceedings*. Wellington: Ministry of Economic Development, 2008, pp. 1–17.

[5] KING, P.R. and G.P. THRASHER. *Cretaceous-Cenozoic Geology and Petroleum Systems of the Taranaki Basin, New Zealand*. Lower Hutt: Institute of Geological and Nuclear Sciences, 1996.

[6] WOOD, R.A., R.H. FUNNELL, P.R. KING, E.R. MATTHEWS, G.P. THRASHER, S.D. KILLOPS and P.G. SCADDEN. Evolution of the Taranaki Basin: hydrocarbon maturation and migration with time. In: *1998 New Zealand Petroleum Conference Proceedings*. Wellington: Ministry of Commerce, 1998. pp. 307–316.

[7] STROGEN, D.P., K.J. BLAND, J.R. BAUR and P.R. KING. Regional Paleogeography and implications for petroleum prospectivity in Taranaki Basin, New Zealand. In: *AAPG Annual Convention and Exhibition: April 22–25, 2012, Long Beach, California, USA*.

[8] JIAN, X. and S. ZHU. Predictive deconvolution for attenuation of multiple reflections in marine seismic data processing. *Journal of Coastal Research: Special Issue 73 – Recent Developments of Port and Ocean Engineering*. 2015, 73, pp. 310–314. DOI: https://doi.org/10.2112/SI73-054.1

[9] LEITE, L.W.B. and W.W.S. VIEIRA. Automatic seismic velocity analysis based on nonlinear optimization of the semblance function. *Journal of Applied Geophysics*. 2018, 161, pp. 182–192. DOI: https://doi.org/10.1016/j.jappgeo.2018.12.015

[10] DIX, C.H. Seismic velocities from surface measurements. *Geophysics*. 1955, 20(1), pp. 68–86. DOI: https://doi.org/10.1190/1.1438126

[11] SCHNEIDER, W.A. The common depth point stack. *Proceedings of the IEEE*. 1984, 72(10), pp. 1238–1254. DOI: https://doi.org/10.1109/PROC.1984.13014

[12] YILMAZ, O. *Seismic Data Processing*. Society of Exploration Geophysicists, 1987. ISBN: 9780931830464.

[13] SHERIFF, R.E. and L.P. GELDART. *Exploration Seismology*. Vol. 1 & 2. CUP, 1982.

[14] GRIPPA, A., A. HURST, G. PALLDINO, D. IACPINI, L.I. ISABELLE and M. HUUSE. Seismic imaging of complex geometry: Forward modeling of sandstone intrusions. *Earth and Planetary Science Letters*. 2019, 513, pp. 51–63. DOI: https://doi.org/10.1016/j.epsl.2019.02.011

[15] BANCROFT, J.C. *A Practical Understanding of Pre- and Poststack Migration*. Vol. 1 & 2. Society of Exploration Geophysicists, 1998.

[16] ANDERTON, P.W. Structure and evolution of the South Wanganui Basin, New Zealand. *New Zealand Journal of Geology and Geophysics*. 1981, 24(1), pp. 39–63. DOI: https://doi.org/10.1080/00288306.1981.10422697

[17] PALMER, J.A. and P.B. ANDREWS. Cretaceous-Tertiary sedimentation and implied tectonic controls on the structural evolution of Taranaki Basin, New Zealand. *Sedimentary Basins of the World, Vol. 2: South Pacific Sedimentary Basins*, edited by P. F. Balance. Amsterdam: Elsevier, 1993, pp. 309–328.

[18] MORTIMER, N., A.J. TULLOOCH and. T.R. IRELAND. Basement geology of Taranaki and Wanganui basins, New Zealand. *New Zealand Journal of Geology and Geophysics*. 1997, 40(2), pp. 223–236. DOI: https://doi.org/10.1080/00288306.1997.9514754

[19] STAGPOOLE, V.M. *A geophysical study of the northern Taranaki Basin, New Zealand*. Wellington, 1997. Ph.D. thesis. Victoria University of Wellington.

[20] STAGPOOLE, V.M., S.L. BENNIE, H.M. BIBBY, M.R. INGHAM and S. DRAVITZKI. Upper crustal structure of the Taranaki Fault imaged by a magnetotelluric study. *Geological Society of New Zealand Miscellaneous Publication 122A*. Wellington: Massey University, 2006. pp. 80– 81.

[21] STAGPOOLE, V.M. and A. NICOL. Regional structure and kinematic history of a large subduction back thrust: Taranaki Fault, New Zealand. *Journal of Geophysical Research*. 2008, 113(B1), pp. 1–19. DOI: https://doi.org/10.1029/2007JB005170